



UNIVERSITY OF LEEDS

This is a repository copy of *Sintering behaviour and ac conductivity of dense $Ce_{0.8}Gd_{0.2}O_{1.9}$ solid electrolyte prepared employing single-step and two-step sintering process.*

White Rose Research Online URL for this paper:
<http://eprints.whiterose.ac.uk/99450/>

Version: Accepted Version

Article:

Wang, Z, Kale, GM and Tang, X (2014) Sintering behaviour and ac conductivity of dense $Ce_{0.8}Gd_{0.2}O_{1.9}$ solid electrolyte prepared employing single-step and two-step sintering process. *Journal of Materials Science*, 49 (8). pp. 3010-3015. ISSN 0022-2461

<https://doi.org/10.1007/s10853-013-7994-1>

© Springer Science+Business Media New York 2014. This is an author produced version of a paper published in *Journal of Materials Science*. Uploaded in accordance with the publisher's self-archiving policy. The final publication is available at Springer via <http://dx.doi.org/10.1007/s10853-013-7994-1>.

Reuse

Unless indicated otherwise, fulltext items are protected by copyright with all rights reserved. The copyright exception in section 29 of the Copyright, Designs and Patents Act 1988 allows the making of a single copy solely for the purpose of non-commercial research or private study within the limits of fair dealing. The publisher or other rights-holder may allow further reproduction and re-use of this version - refer to the White Rose Research Online record for this item. Where records identify the publisher as the copyright holder, users can verify any specific terms of use on the publisher's website.

Takedown

If you consider content in White Rose Research Online to be in breach of UK law, please notify us by emailing eprints@whiterose.ac.uk including the URL of the record and the reason for the withdrawal request.



eprints@whiterose.ac.uk
<https://eprints.whiterose.ac.uk/>

Sintering behavior and ac-conductivity of dense $\text{Ce}_{0.8}\text{Gd}_{0.2}\text{O}_{1.9}$ solid electrolyte prepared employing single step and two-step sintering process

Zihua Wang,^a Girish M. Kale,^{a*} and Xue Tang^b

^a Institute for Materials Research, School of Process, Environmental and Materials Engineering, University of Leeds, Leeds LS2 9JT, U.K.

^b Institute of Particle Science and Engineering, School of Process, Environmental and Materials Engineering, University of Leeds, Leeds LS2 9JT, U.K.

*Author for all correspondences: g.m.kale@leeds.ac.uk (E); 0044-113-3432805 (T)

ABSTRACT

High density sub-microcrystalline $\text{Ce}_{0.8}\text{Gd}_{0.2}\text{O}_{1.9}$ (CGO) ceramics using an unconventional Two Step Sintering (TSS) process have been successfully obtained. Impedance spectroscopy has been used to measure conductivity of CGO samples between 283 and 422 °C. The CGO ceramic samples sintered using TSS process have been found to deliver superior physical and electrical properties compared to those processed employing Single Step Sintering (SSS) process.

KEYWORDS: Solid oxide fuel cell (SOFC), Cerium-gadolinium oxide, Sintering behaviour, Microstructure, Impedance spectroscopy and Ionic conductivity

1. Introduction

In order to achieve long term performance stability and to widen the material selections, solid oxide fuel cell (SOFC) technologies are moving away from traditional high operating

temperature of 1000 °C to intermediate or low temperatures ranging from 500~800 °C [1-3]. One of the ways to circumvent the problems such as lower ionic conductivity and high electrode over-potential that prevails at intermediate and low temperatures in SOFCs is to use solid electrolyte thin films with high ionic conductivity and high chemical stability in oxygen potential gradient prevailing in an SOFC across its electrolyte. This can be achieved through the use of high conductivity thin film solid electrolyte such as gadolinium doped ceria ($\text{Ce}_{0.8}\text{Gd}_{0.2}\text{O}_{1.9}$, CGO) in intermediate or low operating temperature of SOFC [4,5].

In the previous investigations by Kale and co-workers [6-9], it has been shown that the nanoparticulate compacts exhibit the ability to sinter rapidly to high density at low temperatures as a result of high surface area of nanopowders. Furthermore, it has been noticed that the sintered ceramic having nanocrystalline grains tend to exhibit high fracture toughness. However, it is well known that the rate of grain growth during sintering depends on sintering temperature and dwell time [6-9]. In this study, the sintering behavior and ionic conductivity of CGO has been evaluated by using conventional Single Step Sintering (SSS) and a Two Step Sintering (TSS) process recently developed by Chen and Wang [10]. A comparison is then drawn between the influence of the two sintering techniques on the physical and electrical properties of CGO. The microstructures of these samples are observed by Scanning Electron Microscopy (SEM) and the electrical conductivities are measured by Impedance Spectroscopy. Details of the research work and its findings are described in this communication.

2. Experimental

High purity nanopowders of $\text{Ce}_{0.8}\text{Gd}_{0.2}\text{O}_{1.9}$ (CGO) were synthesised using a novel sol-gel method based on maltose and pectin [11], akin to jam making process employed in food industry. The CGO nanopowders obtained after calcination at 500 °C for 2 hours are about 10 nm. The finely

powdered CGO sample was firstly compacted into disc by pressing nanopowders in a uniaxial die at approximately 14 MPa pressure, and then pressed at 300 MPa pressure in a cold isostatic press for further compaction. The relative density (RD) of the green body samples were about 40%. These pellet samples were subsequently sintered in air using SSS and TSS process, respectively.

In SSS, different sample pellets were sintered separately at 1250, 1300, 1350, 1400, 1450, 1500 and 1550 °C for 2 hours in static air at ambient pressure. The heating and cooling rate was maintained at 3 °C min⁻¹ during the sintering process.

In TSS process, different samples were first heated up to T₁ (1400 or 1450 °C) with temperature increasing at the rate of 3 °C min⁻¹ to the set temperature. Without allowing any annealing time, the temperatures were then decreased immediately to T₂ (1350 or 1400 °C) respectively at the rate of 50 °C min⁻¹, for annealing period of 15 or 20 hours, respectively. These two samples are denoted as 1400-1350°C-15hrs (TSS1) and 1450-1400°C-20hrs (TSS2), respectively. The density of all the sintered samples was measured by the Archimedes principle.

Microstructures of the fractured surface of the sintered CGO compacts were observed by Scanning Electron Microscopy (FEG-SEM LEO Gemini 1530). The alternating current (ac) conductivity measurements of the CGO pellets were performed using an impedance analyzer (SI-1260, Schlumberger Technology GmbH, Munich, Germany) in the frequency range 1 Hz~3.2 MHz. The two flat surfaces of the sintered pellets were coated with Pt paint to provide good electrical contacts. In order to provide a good adhesion between Pt and CGO pellets, the Pt-coated CGO pellets were heat treated at 800 °C for 30 mins. The samples were spring loaded in a quartz assembly for the measurement of ac-conductivity as a function of temperature between 283 to 422 °C, using a programmable horizontal tube furnace (Lenton Thermal Designs Ltd,

Market Harborough, UK). The assembly including the measuring leads was earthed to avoid any electrical interference on the measurements by housing it in a Faraday cage. An additional thermocouple placed close to the sample was used to measure the actual sample temperature during the measurements.

3. Results and Discussion

The conventional sintering practice for CGO is to heat the powder compact at elevated temperature for a desired length of time to ensure that the maximum density of the ceramic compact is achieved. As shown in Figure 1 SSS, the relative density of CGO samples sintered in this way increases continuously with the heat treatment temperature, from 1250 °C to 1550 °C, with 2 hours of annealing time. The specimens begin to show an evident densification (~68%) at temperature higher than 1350 °C and exhibit a maximum density of about 92% after sintering at 1550 °C for 2 hours as seen in Figure 1. Furthermore, the increment in density between 1450 – 1550 °C is only about 3% signifying that a saturation point has been reached for the densification of CGO. According to the investigation by Chen and Wang [10], a success of two-step sintering strongly depends on the choice of temperatures T_1 and T_2 where T_1 is usually greater than T_2 . Samples should be sintered to a selected high temperature T_1 to yield a relative density greater than 75%, at which stage all pores became subcritical and unstable against shrinkage. After rapidly cooling down and annealing the samples for prolonged duration at T_2 , high density ceramics without significant grain growth could be obtained where the sintering due to grain boundary or volume diffusion dominates while the grain boundary motion is relatively frozen [10]. As seen in Figure 1, CGO sample initially heated to 1400 °C and subsequently held at 1350 °C for 15 hours yield samples having ~94% relative density denoted as TSS1. Similarly, in another experiment, the first sintering step was carried out at 1450 °C followed by annealing at

1400 °C for 20 hours yield almost full densification (~99% relative density) without significant grain growth, denoted as TSS2 in Figure 1.

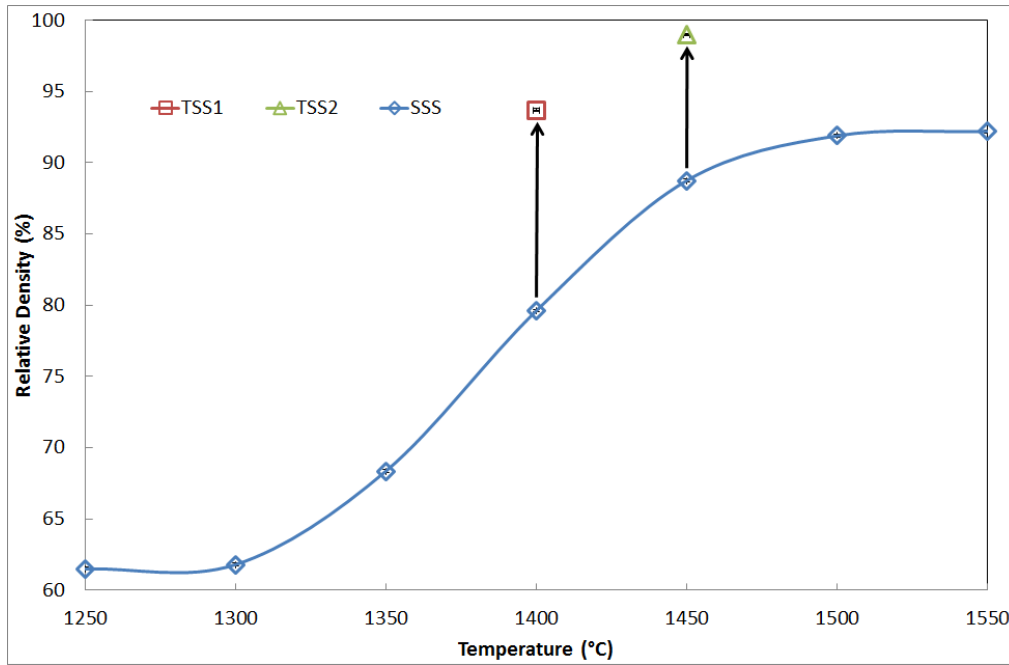


Fig. 1 Densification curve of CGO samples after Single Step Sintering (SSS) and Two-Step Sintering (TSS), respectively.

The microstructure of the fractured surface of CGO samples sintered under different conditions are shown in Figure 2. In an SSS process, final stage densification is always accompanied by rapid grain growth. It is clearly seen in Figure 2A to 2D that as temperature increases from 1350 °C to 1500 °C, the average grain size increases from ~100 nm to ~2 μm, respectively. In contrast to this, smaller grain sizes about 500 nm and 1 μm are obtained after TSS process, as seen in Figure 2E and 2F, respectively. Smaller CGO grain size with higher density is likely to give rise to enhanced fracture toughness and hence will improve the tolerance limit of solid electrolyte in SOFC against thermal shock and thermal cycling damage [12].

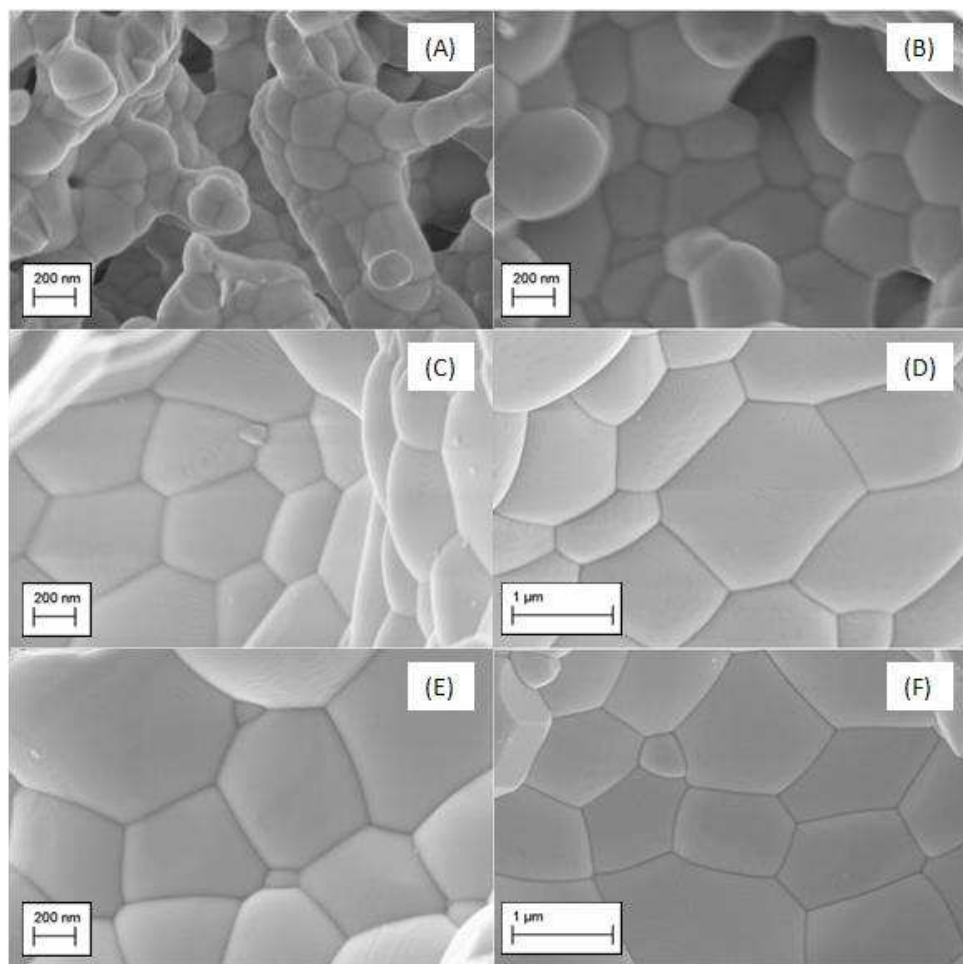
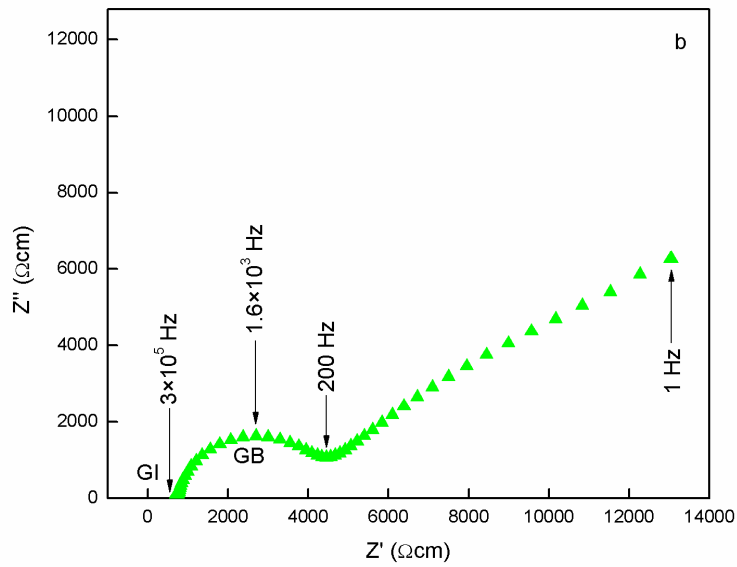
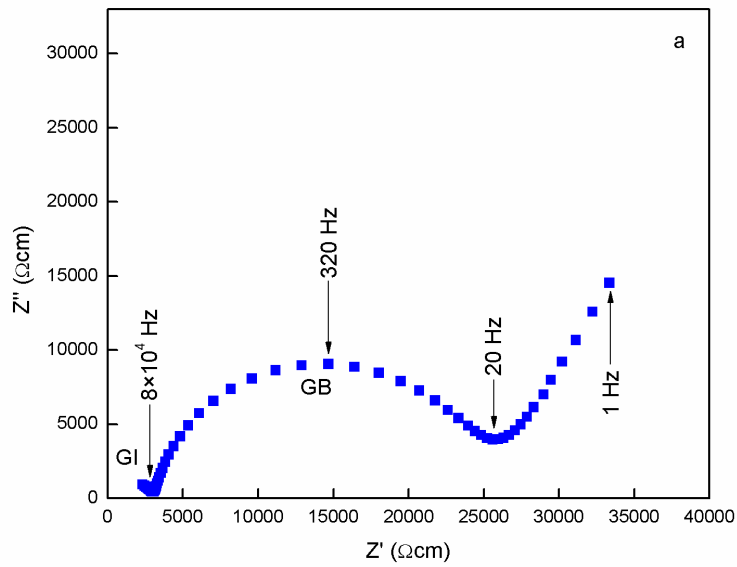


Fig. 2 SEM images of CGO sintered at different conditions: (A) 1350°C-2hrs, (B) 1400°C-2hrs, (C) 1450°C-2hrs, (D) 1500°C-2hrs, (E) 1400°C-1350°C-15hrs (TSS1) and (F) 1450°C-1400°C-20hrs (TSS2), respectively.

The ionic, grain boundary and total conductivity of samples sintered using both the sintering processes (SSS and TSS) was measured by a four-probe impedance analysis. Figure 3 shows the selected impedance diagrams at 283, 331 and 373 °C in air at ambient pressure, respectively of the dense submicron grain CGO TSS2 (1450°C-1400°C-20hrs) sample. Clearly, the various electrical processes such as the grain boundary, bulk and electrode polarization effects can be identified from the data measured at 373 °C as shown in Figure 3a however as temperature increases the semicircle due to bulk conduction process seem to become progressively less

prominent as seen in Figure 3b and 3c. This is a common feature of most of the ion conducting ceramic materials.



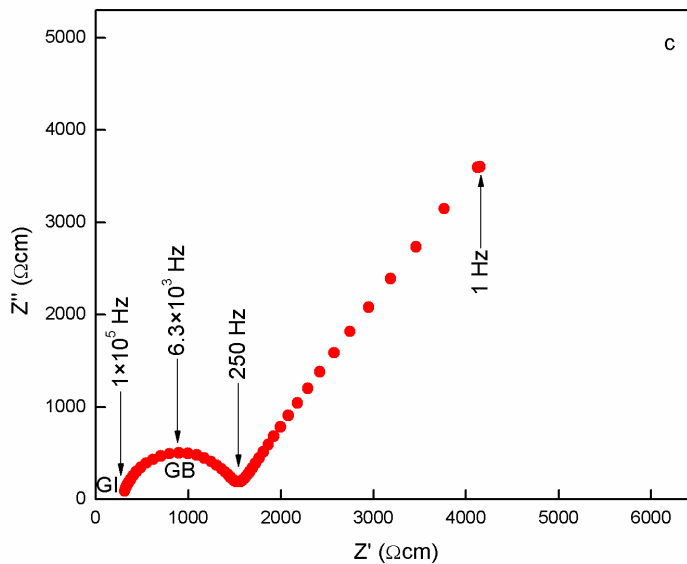
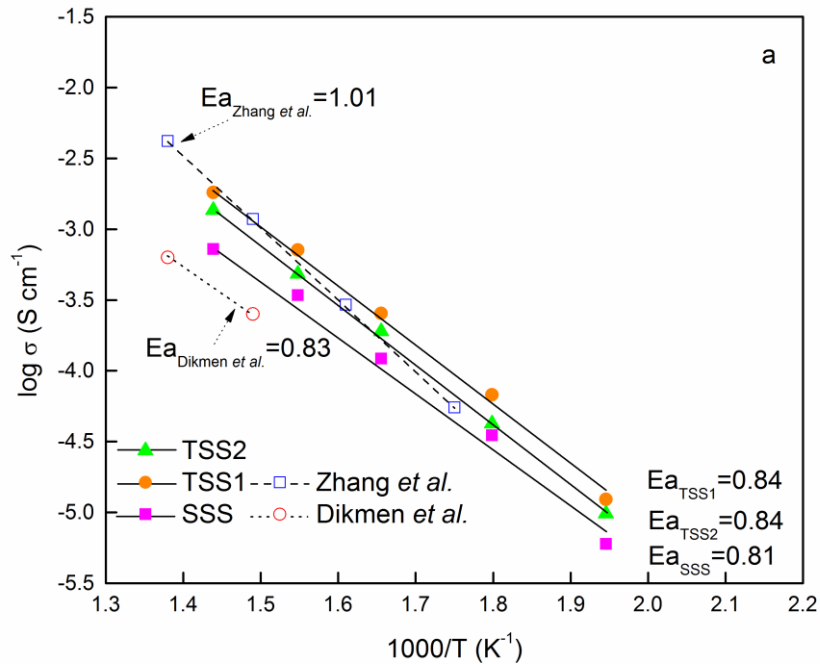
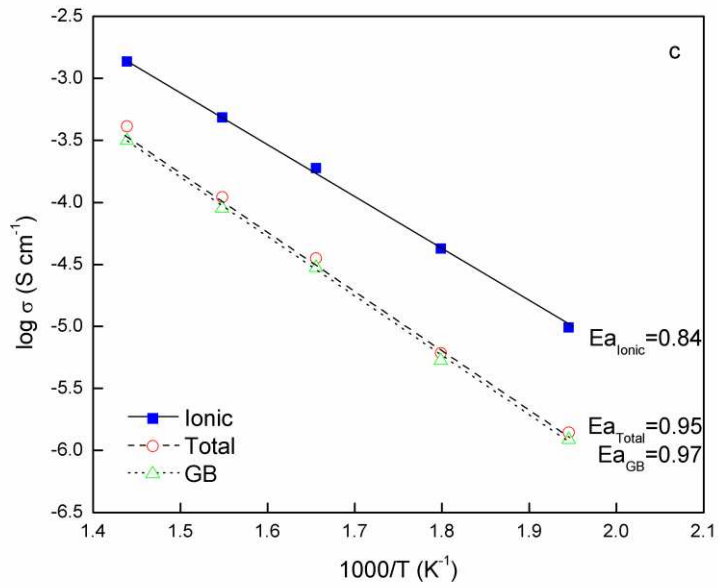
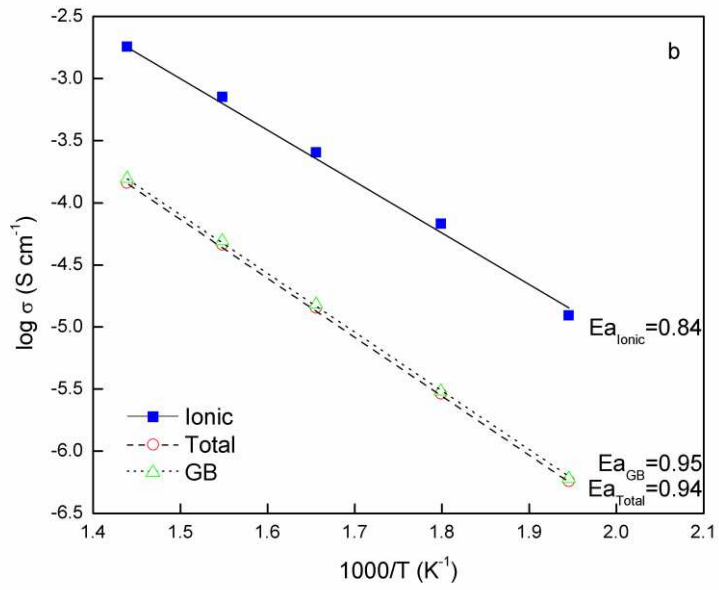


Fig. 3 Impedance diagrams of the data measured at (a) 283 °C, (b) 331 °C and (c) 373 °C in air of CGO sintered at 1450°C-1400°C-20hrs (TSS2), respectively. The GI and GB arcs denoted in the diagrams, respectively stand for grain interior and grain boundary effects.

The measured impedance data shown in Figure 3a-3c as a function of temperature were fitted using ZVIEW software (Scribner Inc, USA) to a series of RC-parallel equivalent circuits to obtain the grain interior and grain boundary conductivity of the sintered CGO samples. Figure 4 shows the variation of the logarithm of conductivity of the sintered CGO samples as a function of the reciprocal of absolute temperature from 514 K to 695 K in static air condition at ambient pressure. The Arrhenius plots in Figure 4a indicates that the highest value of the activation energies for the ionic conductivity are 0.84 eV of CGO samples heat treated by TSS process, respectively. These values agree reasonably well with the literature data [13-15], which are lower compared with the results obtained by Zhang et al [13] and comparable with the results of Dikmen et al [14] but lower than our own previous measurements [15]. This may in part be due

to the higher density (94~99%) of the samples investigated in this study compared to (91~93%) dense samples used in the previous study [15]. The activation energies of around 0.84 eV, 0.95 eV and 0.94 eV, respectively have been obtained from the measured data in this investigation corresponding to the bulk ($E_{a_{ionic}}$), grain boundary ($E_{a_{GB}}$) and total ($E_{a_{Total}}$) conductivities of CGO TSS1 samples (see Figure 4b). Similarly, the activation energies of around 0.84 eV, 0.97 eV and 0.95 eV, respectively have been obtained from the measured values of the bulk ($E_{a_{ionic}}$), grain boundary ($E_{a_{GB}}$) and total ($E_{a_{Total}}$) conductivities of CGO TSS2 samples (see Figure 4c). The activation energy for conduction in bulk is lower than grain boundary in both TSS1 and TSS2 samples probably because more energy is required to transport the oxide anions between different grains compared to that within the grains due to possible imperfections at the grain boundaries. Similar trend is observed in the results obtained from the samples sintered using the SSS process as shown in Figure 4d.





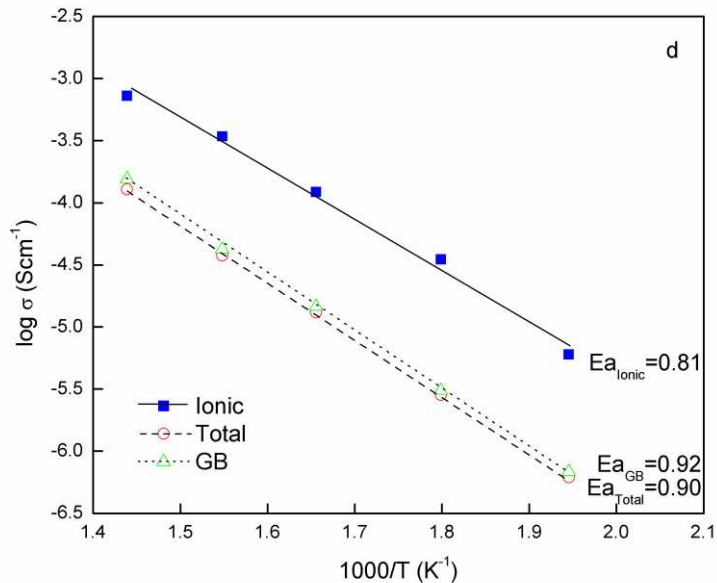


Fig. 4 Arrhenius plots of conductivity of CGO sintered at different conditions: (a) GI conductivity of CGO compared with Zhang et al [13] and Dikmen et al [14] data, (b) GI/GB/Total conductivity of CGO sintered at 1400°C-1350°C-15hrs (TSS1), (c) GI/GB/Total conductivity of CGO sintered at 1450°C-1400°C-20hrs (TSS2), (d) GI/GB/Total conductivity of CGO sintered at 1500°C-2hrs (SSS), respectively. Values of E_a are in eV.

As shown in Table 1, the ionic conductivities of the bulk CGO ceramic material at 422 °C obtained by TSS1, TSS2 and SSS process are $1.66 \times 10^{-2} \text{ Scm}^{-1}$, $1.36 \times 10^{-3} \text{ Scm}^{-1}$ and $7.24 \times 10^{-4} \text{ Scm}^{-1}$, respectively. Clearly, higher ionic conductivity values are observed in TSS1 and TSS2 samples compared with SSS sample. Furthermore, both the grain boundary and total conductivities obtained from sintered CGO samples using TSS heat treatment process are higher compared with normal SSS process (See Table 1). This clearly suggests that the CGO ceramic samples sintered using TSS process delivers superior physical and electrical properties compared to those processed employing SSS process. Additionally, it can be seen in Table 1 that the total conductivity of TSS2 sample ($3.16 \times 10^{-4} \text{ Scm}^{-1}$) is greater than that of TSS1 sample (1.45×10^{-4}

Scm^{-1}). This is probably because of the presence of smaller grain size and hence large density of grain boundaries contributing to relatively higher resistance for ionic conduction in TSS1 than in TSS2 sample.

Table 1 Bulk (GI), grain boundary (GB) and total conductivity measured at 422 °C and, relative density and average grain size measured at ambient temperature of CGO solid solution heat treated by 1400°C-1350°C-15hrs (TSS1), 1450°C-1400°C-20hrs (TSS2) and 1500°C-2hrs (SSS) processes.

	TSS1	TSS2	SSS
σ_{GI} (S cm^{-1})	1.66×10^{-2}	1.36×10^{-3}	7.24×10^{-4}
σ_{GB} (S cm^{-1})	1.57×10^{-4}	4.11×10^{-4}	1.56×10^{-4}
σ_{Total} (S cm^{-1})	1.45×10^{-4}	3.16×10^{-4}	1.28×10^{-4}
Relative Density (%)	93.7±0.012	99.0±.001	91.9±0.007
Aver. Grain Size (μm)	~0.5	~1	~2

4. Conclusion

In this investigation, high density bulk sub-microcrystalline CGO ceramics have been successfully obtained using an unconventional Two Step Sintering (TSS) strategy which offers the advantage of smaller grain size while increasing density from about 75% to 94~99% of theoretical value at low sintering temperatures between 1400 – 1450 °C. Using nanosized powders, high density CGO ceramics with a typical grain size of 500 nm and 1 μm were obtained by following TSS1 and TSS2 sintering profile, respectively. Smaller grain size obtained by TSS relative to the SSS process is likely to improve the mechanical performance of ceramic solid electrolyte against thermal shock or thermal cycling in SOFC application.

The measured bulk, grain boundary and total conductivity of CGO samples heat treated by different methods have been measured between 283 and 422 °C. Bulk conductivity value of 1.66×10^{-2} and $1.36 \times 10^{-3} \text{ S cm}^{-1}$ at 422 °C in air at ambient pressure has been obtained for TSS1 and TSS2 CGO samples, respectively. These values are 1~2 order of magnitude higher compared with the one ($7.24 \times 10^{-4} \text{ S cm}^{-1}$) obtained for the identical CGO composition sample sintered using SSS process. The relative density of the samples sintered at 1400 – 1450 °C by TSS process is greater by 12 – 15% compared to the samples sintered by SSS process at the same temperature.

The properties such as high density, high ionic conductivity, low sintering temperature and smaller grain size obtained by TSS would certainly make this a preferred manufacturing method of processing CGO for IT-SOFC application.

Reference

1. Doshi R, Richards VL, Charter JD, Wang XP, Krumpelt M (1999) Development of solid-oxide fuel cells that operate at 500 degrees C, *J Electrochem Soc* 146:1273-1278.
2. Steele BCH (2000) Materials for IT-SOFC stacks 35 years R&D: the inevitability of gradualness, *Solid State Ionics* 134:3-20.
3. Steele BCH (2000) Kinetic parameters influencing the performance of IT-SOFC composite electrodes, *Solid State Ionics* 135:445-450.
4. Leng YJ, Chan SH, Jiang SP, Khor KA (2004) Low-temperature SOFC with thin film GDC electrolyte prepared in situ by solid-state reaction, *Solid State Ionics* 170:9-15.
5. Sun C, Li H, Chen LQ (2012) Nanostructured ceria-based materials: synthesis, properties, and applications, *Energy Environ Sci* 5:8475-8505.

6. Zhen QA, Kale GM, He WM, Liu JQ (2007) Microwave plasma sintered nanocrystalline $\text{Bi}_2\text{O}_3\text{-HfO}_2\text{-Y}_2\text{O}_3$ composite solid electrolyte, *Chem Mater* 19:203-210.
7. Lee HY, Kale GM (2008) Hydrothermal Synthesis and Characterization of Nano- TiO_2 , *Int J Appl Ceram Technol* 5:657-665.
8. Wang XT, Kale GM (2008) Microwave sintering of YSZ electrolyte materials for SOFC, *Key Eng Mater* 268:238-240.
9. Zhen QA, Kale GM, Shi G, Li R, He WM, Liu JQ (2005) Processing of dense nanocrystalline $\text{Bi}_2\text{O}_3\text{-Y}_2\text{O}_3$ solid electrolyte, *Solid State Ionics* 176:2727-2733.
10. Chen IW, Wang XH (2002) Sintering dense nanocrystalline ceramics without final-stage grain growth, *Nature* 404:168-171.
11. Wang ZH, Comyn TP, Ghadiri M, Kale GM (2011) Maltose and Pectin assisted sol-gel production of $\text{Ce}_{0.8}\text{Gd}_{0.2}\text{O}_{1.9}$ solid electrolyte nanopowders for solid oxide fuel cells, *J Mater Chem* 21:16494-16499.
12. Bellon O, Sammes NM, Staniforth J (1998) Mechanical properties and electrochemical characterisation of extruded doped cerium oxide for use as an electrolyte for solid oxide fuel cells, *J Power Sources* 75:116-121.
13. Zhang TS, Ma J, Kong LB, Hing P, Leng YJ, Chan SH, Kilner JA (2003) Preparation and electrical properties of dense submicron-grained $\text{Ce}_{0.8}\text{Gd}_{0.2}\text{O}_{2-\delta}$ ceramics, *J Mater Sci Lett* 22:1809-1811.
14. Dikmen S, Shuk P, Greenblatt M, Gocmez H (2002) Hydrothermal synthesis and properties of $\text{Ce}_{1-x}\text{Gd}_x\text{O}_{2-\delta}$ solid solutions, *Solid State Sci* 4:585-590.

15. Wang ZH, Kale GM, Ghadiri M (2012) Synthesis and characterization of $Ce_xGd_{1-x}O_{2-\delta}$ nanopowders employing an alginate mediated ion-exchange process, Chem Eng J 198-199:149-153.